

## Eddy-to-mean energy transfer in geophysical turbulent jet flows

Jaak Heinloo and Aleksander Toompuu

Marine Systems Institute at Tallinn University of Technology, Akadeemia tee 21, 12618 Tallinn, Estonia; heinloo@phys.sea.ee, alex@phys.sea.ee

Received 12 June 2006, in revised form 19 January 2007

**Abstract.** The eddy-to-mean energy transfer in turbulent flows is discussed. The discussion proceeds from the theory of rotationally anisotropic turbulence (RAT theory). It is shown that the rotational viscosity introduced in the RAT theory to quantify the interaction between the orientated (large-scale) turbulence constituent and the average flow can explain the eddy-to-mean energy transfer. The theoretical predictions are particularized for a jet stream model in a geophysical situation and compared with the data measured in the Gulf Stream transverse sections along 26°N (Florida Straits) and along 35°N (off Onslow Bay). The suggested model agrees with the measured data and points to a substantial difference in the data interpretation within the suggested model and within the conventional turbulence mechanics.

**Key words:** turbulence, negative viscosity, geophysical jets, Gulf Stream.

### 1. INTRODUCTION

The observational evidence of the eddy-to-mean (ETM) energy transfer accompanied by the upgradient momentum transport in turbulent flows [<sup>1–4</sup>] reveals a major inconsistency in the conventional turbulence mechanics (CTM). The CTM agrees with the observed phenomenon only if the negative shear viscosity coefficient (not accepted by the physics of viscosity) is allowed. This paper shows that the theory of rotationally anisotropic turbulence (RAT theory [<sup>5–7</sup>]) overcomes the indicated inconsistency in the CTM. Unlike the CTM, which explains the phenomenon as forced by the (turbulent) shear viscosity, the RAT theory explains the phenomenon as forced by the (positive) rotational viscosity, introduced within that theory to quantify the effect of shear in relative rotation.

The discussion starts with an introduction to the RAT theory (Section 2), which outlines some essential aspects like the interrelation between the RAT theory and the CTM, insufficiently addressed in earlier RAT treatments. The

physics of the ETM energy transfer in turbulent flows is explained in Section 3. Section 4 particularizes this explanation on the model of a jet stream in a geophysical situation. In Section 5 the theoretical predictions of the model are compared with the data measured in the Gulf Stream along transverse sections at about 26°N (Florida Straits) and 35°N (off Onslow Bay) [8]. It is shown that the model explains the marked difference between the turbulence regimes on the cyclonic and anticyclonic sides of the stream. Unlike the approach in [9], treating the phenomenon as specific to the considered region of the Gulf Stream, the suggested model treats the phenomenon as an effect common to geophysical jet streams independent from the particularities of their occurrence location.

The interpretation of the observed data within the CTM would state the domination of the ETM energy transfer in almost the entire cross-sectional area of the stream and would presume the presence of a substantial turbulent energy source in the region. It is shown that the same data, if interpreted from the point of view of the RAT theory, show a rather marginal role of the ETM energy transfer in the area. The majority of the energy exchange is directed from the mean flow to the turbulence within this interpretation and no additional energy source is required for the data explanation.

The discussion of the energy transfer processes in geophysical turbulent jets presented in this paper complements earlier oceanographic applications of the RAT theory [10-15].

## 2. INTRODUCTION TO THE RAT THEORY

The CTM proceeds from presenting the velocity of the turbulent flow field  $\mathbf{v}$  as the sum  $\mathbf{v} = \mathbf{u} + \mathbf{v}'$ , where  $\mathbf{u} = \langle \mathbf{v} \rangle$ , in which (and henceforth) angular brackets denote statistical averaging, and  $\mathbf{v}'$  is the fluctuating constituent of the flow velocity. The flow description is then realized within the average momentum (Reynolds) equation with the symmetric turbulent stress tensor  $\sigma_{ij} = -\rho \langle v'_j v'_i \rangle$  ( $\rho$  is the medium density,  $v'_i$  and  $v'_j$  are components of  $\mathbf{v}'$ , the Latin indices  $i, j$  obtain the values 1, 2, and 3) and the equation for the turbulence energy  $K = \frac{1}{2} \langle v'^2 \rangle$ . The symmetry of the turbulent stress tensor presumes the probability distribution invariance under commutation of its arguments  $v'_j$  and  $v'_i$ .

The RAT theory [5-7] generalizes the CTM to account for the preferred orientation of the eddy rotation. The generalization is realized by including the curvature radius  $\mathbf{R}$  of  $\mathbf{v}'$  streamline into the set of arguments of the applied probability distribution. The inclusion allows us to determine at each flow field point the quantity

$$\mathbf{M} = \langle \mathbf{v}' \times \mathbf{R} \rangle, \quad (1)$$

having the physical sense of the internal moment of momentum (angular momentum, spin) of the turbulent flow field and expressing a local measure of the average effect of a preferred orientation of turbulent eddy rotation.

As a corollary of the condition  $\mathbf{M} \neq 0$  (turbulent flows of this type are called rotationally anisotropic) the turbulence energy  $K = \frac{1}{2} \langle v'^2 \rangle$  becomes split into the sum

$$K = K^\Omega + K^0 \quad (2)$$

in which  $K^\Omega = \frac{1}{2} \mathbf{M} \cdot \boldsymbol{\Omega}$  and  $K^0 = \frac{1}{2} \langle \mathbf{M}' \cdot \boldsymbol{\Omega}' \rangle$ , where  $\boldsymbol{\Omega} = \langle \mathbf{v}' \times \mathbf{R} / R^2 \rangle$ ,  $\mathbf{M}' = \mathbf{v}' \times \mathbf{R} - \mathbf{M}$  and  $\boldsymbol{\Omega}' = \mathbf{v}' \times \mathbf{R} / R^2 - \boldsymbol{\Omega}$  while  $R = |\mathbf{R}|$ . The quantity  $\boldsymbol{\Omega}$  has the sense of the average angular velocity of eddies' rotation, determined as independent from the average velocity  $\mathbf{u}$ . The energy  $K^\Omega$  in (2) characterizes the orientated turbulence constituent contributing to  $\mathbf{M}$ , and  $K^0$  characterizes the turbulence constituent not contributing to  $\mathbf{M}$ . The motion description of turbulent media with the condition  $\mathbf{M} \neq 0$  is formulated within the equations for the average momentum (the Reynolds equation) with an asymmetric turbulent stress tensor, for the moment of momentum  $\mathbf{M}$ , and for energy  $K^0$ .

The distinction between the turbulence constituents contributing and not contributing to  $\mathbf{M}$  is coupled with the difference in the interaction of the constituents with the average flow. The difference is revealed in the asymmetry of the turbulent (Reynolds) stress tensor with the symmetric constituent describing the interaction between the average flow and the turbulence constituent with energy  $K^0$  and with the antisymmetric constituent describing the interaction between the average flow and the turbulence constituent with  $\mathbf{M}$ ,  $\boldsymbol{\Omega}$ , and energy  $K^\Omega$ . The RAT theory explains the asymmetry of the turbulent stress tensor by the non-invariance of the applied probability distribution in respect to commutation of its arguments  $v'_j$  and  $v'_i$ .

In full compliance with the continuum mechanics [16,17] the antisymmetric constituent of the turbulent stress tensor vanishes, together with  $\mathbf{M}$ ,  $\boldsymbol{\Omega}$ , and  $K^\Omega$  when either  $\mathbf{R}$  is not included into the set of arguments of the applied probability distribution or when there is no preferred orientation of eddy rotation. Then the RAT theory is reduced to the CTM. However, there is a considerable difference between the two cases of the reduction of the RAT theory to the CTM, leading to a difference in the interpretation of the relationship between the CTM and the RAT theory. The first interpretation follows from the orthodox treatment of the CTM. If the symmetry of the turbulent stress tensor is postulated, then any possibility of accounting for a preferred orientation of eddy rotation is constitutively excluded and the relationship between the CTM and the RAT theory is considered contradictory. The second interpretation (suggested by the RAT theory) appreciates the situation described within the CTM as limited by the adopted assumption about the symmetric stress tensor. It does not refute the CTM but merely restricts its competence by the description of the turbulence constituent with the symmetric stress tensor and energy  $K^0$ .

Besides the CTM, the RAT theory also comprises the idea of the 1970s to incorporate the equation of the moment of momentum (angular momentum) into the turbulence description setup [18-21], discussed in the context of possible applications of the hydrodynamics of micropolar continua developed in the

1960s–1970s [22–25]. It also allows inclusion of some aspects of the Richardson–Kolmogoroff concept about the cascading turbulence [26,27] into the turbulence mechanical description setup. The objective of the suggested approach coincides with the objective of large-eddy simulation methods applied to the turbulence description [28–30]. The main difference is that the suggested approach (RAT theory) accounts for effects of the large-scale turbulence immediately in terms of average fields.

### 3. PHYSICS OF THE EDDY-TO-MEAN ENERGY TRANSFER IN TURBULENT FLOWS

Consider work  $W$  done by the turbulent stresses,

$$W = \sigma_{ij,j} u_i = \nabla \cdot \mathbf{h} - Q,$$

where  $\mathbf{h}$ , defined by its components

$$h_j = \sigma_{ij} u_i, \quad (3)$$

describes the turbulent flux of energy  $K = \frac{1}{2} u^2$  and

$$Q = \sigma_{ij} u_{i,j} \quad (4)$$

describes the energy transfer between the average flow and the turbulence. For  $Q > 0$  the average flow feeds energetically the turbulence and for  $Q < 0$  the energy is transferred from eddies to the mean flow. The latter process is accompanied by the upgradient transport of the momentum. After division of the turbulent stress tensor in (4) into the sum of symmetric and antisymmetric constituents expression (4) can be represented as the sum

$$Q = Q^s + Q^{as},$$

where  $Q^s = \sigma_{(ij)} u_{i,j}$  in which  $\sigma_{(ij)} = \frac{1}{2}(\sigma_{ij} + \sigma_{ji})$  and

$$Q^{as} = -\boldsymbol{\sigma} \cdot \boldsymbol{\omega}, \quad (5)$$

where  $\boldsymbol{\omega} = \frac{1}{2} \nabla \times \mathbf{u}$  is the vorticity and  $\boldsymbol{\sigma}$  is the dual vector to the antisymmetric constituent of the turbulent stress tensor with components  $\sigma_k = e_{kij} \sigma_{ij}$  ( $e_{ijk}$  denotes the Levi-Civita tensor components and the Einstein summation is assumed). The symbol  $Q^s$  describes the energetic interaction between the average flow and the unorientated turbulence constituent with energy  $K^0$ , while  $Q^{as}$  describes the energetic interaction between the average flow and the orientated turbulence constituent with  $\mathbf{M}$ ,  $\boldsymbol{\Omega}$ , and  $K^\Omega$ .

The CTM states that  $\sigma_{ij} = \sigma_{(ij)}$  with  $\sigma_{(ij)}$  parameterized as  $\sigma_{(ij)} = -p \delta_{ij} + 2\mu u_{(i,j)}$ , where  $u_{(i,j)} = \frac{1}{2}(u_{i,j} + u_{j,i})$ ,  $p$  is the pressure,  $\delta_{ij}$  denotes

the components of the unit tensor, and  $\mu$  is the coefficient of turbulent shear viscosity. In this case  $Q = Q^s = \mu u_{(i,j)} u_{(i,j)}$  (the medium is considered incompressible) and the ETM energy transfer ( $Q < 0$ ), together with the upgradient momentum transport, becomes possible only if the negative shear viscosity coefficient  $\mu$  is allowed. Nevertheless, if the momentum gradient is the only forcing of the momentum transport, as it is assumed within the CTM, then the physics of the phenomenon does not foresee the possibility of upgradient momentum transport. Therefore the CTM evidently fails to describe the phenomenon.

Let us treat now the turbulence with a preferred orientation of eddy rotation. We consider the situation within the Richardson–Kolmogoroff concept about the cascading turbulence generation with the large-scale turbulence interacting immediately with the average flow. In this case  $Q^{as}$  dominates over  $Q^s$ , i.e.  $Q$  may be identified with  $Q^{as}$ . In applying to  $\sigma$  the closure [5–7]

$$\sigma = 4\gamma(\Omega - \omega), \quad (6)$$

where  $\gamma \geq 0$  is the coefficient of rotational viscosity, it is evident that, contrary to work  $Q^s$  being negative only for negative  $\mu$ ,  $Q^{as}$  can be either positive or negative for positive  $\gamma$  and therefore the introduction of the rotational viscosity removes the “negative viscosity” problem.

Finally, the situation with  $Q^{as} < 0$  evidently presumes a source of energy for the large-scale (orientated) turbulence constituent other than the average flow. The energy sources could be the magnetic field for the motion of ferromagnetic colloidal systems [2] and magnetic fluids [3] as well as the system rotation in the geophysical hydrodynamics. In the following the latter is specified for geophysical jet flows.

#### 4. A SIMPLE GEOPHYSICAL JET STREAM MODEL

We consider a steady plane flow with  $\mathbf{u} = (0, u(x), 0)$ ,  $\Omega = (0, 0, \Omega)$  in the right-hand Cartesian coordinate system  $(x, y, z)$  with  $z$  directed upwards and with the neglected effect of advection of the moment of momentum  $\mathbf{M} = (0, 0, M = J\Omega)$  ( $J$  is the effective moment of inertia determined from  $M = J\Omega$ ). The vertical projection of the equation for the moment of momentum  $M$  [5–7], written for the motion in a frame rotating with the angular velocity of the Earth’s rotation  $\omega^0 = (0, 0, \omega^0 \sin \vartheta)$ , where  $\omega^0$  is the magnitude of the angular velocity of the Earth’s rotation and  $\vartheta$  is the latitude, is reduced to the balance condition

$$\theta \frac{\partial^2}{\partial x^2} \Omega - \sigma - 4\kappa(\Omega + \omega^0 \sin \vartheta) = 0. \quad (7)$$

In (7),  $\theta > 0$  is the diffusion coefficient of  $M = J\Omega$  and the moment  $4\kappa(\Omega + \omega^0 \sin \vartheta)$ , where  $\kappa > 0$  is the coefficient of cascade scattering, reflects

the joint effect of the Earth's rotation and the decay of  $\mathbf{M}$  in the cascading process. Together with closure (6), Eq. (7) can also be rewritten as

$$\Omega'' - \lambda^2 \Omega = \lambda^2 \left[ -\frac{\gamma}{\gamma + \kappa} \omega + \frac{\kappa}{\gamma + \kappa} \omega^0 \sin \vartheta \right], \quad (8)$$

in which  $\lambda^2 = 4(\gamma + \kappa)L^2/\theta$ , where  $L$  is a constant with the dimension of length, and the apostrophe denotes derivative with respect to the non-dimensional  $x^* = x/L$ . The inverse  $\lambda^{-1}$  determines the non-dimensional diffusion scale of the moment of momentum.

Consider first the situation where the diffusion scale is determined as vanishing, i.e.  $\lambda^{-1} = 0$ , then we find from (8)

$$\Omega = \frac{\gamma}{\gamma + \kappa} \omega - \frac{\kappa}{\gamma + \kappa} \omega^0 \sin \vartheta, \quad (9)$$

and, as a consequence,

$$Q^{\text{as}} = -4\gamma(\Omega - \omega)\omega = 4\frac{\gamma\kappa}{\gamma + \kappa}(\omega + \omega^0 \sin \vartheta)\omega. \quad (10)$$

According to (10), the ETM energy transfer would take place if  $(\omega + \omega^0 \sin \vartheta)\omega < 0$ . The latter condition does not hold for  $\omega^0 = 0$ , therefore the ETM energy transfer can be considered as a specific flow property caused by the system rotation. Let us note that according to (9),  $\omega = 0$  and  $\Omega = -\omega^0 \kappa \sin \vartheta / (\gamma + \kappa)$  beyond the jet area, which agrees with [31] stating a significant turbulence in the ocean interior.

Let us specify  $u = u(x^*)$  in the following as

$$u = u_0 \exp(-x^{*2}). \quad (11)$$

The velocity profile (11) determines vorticity  $\omega$ , moment  $\Omega$ ,  $\sigma$ ,  $Q^{\text{as}}$  and  $h^{\text{as}} = \frac{1}{2}\sigma u$ , which is the  $x$ -component of the flux vector  $\mathbf{h}$  constituent induced by the antisymmetric constituent of the stress tensor, as

$$\omega = -\varepsilon \omega^0 x^* \exp(-x^{*2}), \quad (12)$$

$$\Omega = -\omega^0 \left( \frac{\kappa}{\gamma + \kappa} \sin \vartheta + \varepsilon \frac{\gamma}{\gamma + \kappa} x^* \exp(-x^{*2}) \right), \quad (13)$$

$$\sigma = -4\gamma\omega^0 \frac{\kappa}{(\gamma + \kappa)} (\sin \vartheta - \varepsilon x^* \exp(-x^{*2})), \quad (14)$$

$$Q^{\text{as}} = -4\varepsilon\gamma\omega^{02} \frac{\kappa}{\gamma + \kappa} x^* (\sin \vartheta - \varepsilon x^* \exp(-x^{*2})) \exp(-x^{*2}), \quad (15)$$

$$h_x^{\text{as}} = 2\gamma u_0 \omega^0 \frac{\kappa}{\gamma + \kappa} (\sin \vartheta - \varepsilon x^* \exp(-x^{*2})) \exp(-x^{*2}), \quad (16)$$

where  $\varepsilon$  is the Rossby number [32] specified as  $\varepsilon = u_0/2L\omega^0$ . The dependences (11)–(16) for  $\varepsilon=1$  and  $\gamma=\kappa$  are illustrated in Fig. 1. The profiles for the reduced non-dimensional  $u$ ,  $\Omega$ , and  $\omega$  for  $\vartheta=40^\circ\text{N}$ , defined as  $u^* = u/u_0$ ,  $\Omega^* = \Omega/\omega^0$ , and  $\omega^* = \omega/\omega^0$ , respectively, are represented in Fig. 1a. The field of  $\Omega^* = -\kappa \sin \vartheta / (\gamma + \kappa)$  is determined as homogeneous for the missing jet or sufficiently far from the jet influence. The homogeneity becomes distorted in the jet area (Fig. 1). The distortion is revealed in an increase in  $|\Omega^*|$  on the right (anticyclonic) side of the jet ( $x^* > 0$ ), and in a decrease in  $|\Omega^*|$  on the left (cyclonic) side of the jet ( $x^* < 0$ ), causing this way a substantial difference in the turbulence regimes on either side of the jet. The difference is depicted in Fig. 1b by the profiles of non-dimensional  $\sigma$ ,  $u^2$ ,  $Q^{\text{as}}$ , and  $h_x^{\text{as}}$  defined as  $\sigma^* = \sigma/4\gamma\omega^0$ ,  $u^{*2} = (u/u_0)^2$ ,  $Q^* = Q^{\text{as}}/4\gamma\omega^{02}$ , and  $h^* = h_x^{\text{as}}/2\gamma u_0 \omega^0$ , respectively. For  $x^* < 0$ , vorticity  $\omega^*$  and  $\sigma^*$  have opposite signs and therefore on the left side of the jet  $Q^* > 0$ . On the right side of the jet the signs of  $\omega^*$  and  $\sigma^*$  coincide and  $Q^* < 0$ , highlighting this side of the jet as a region with the

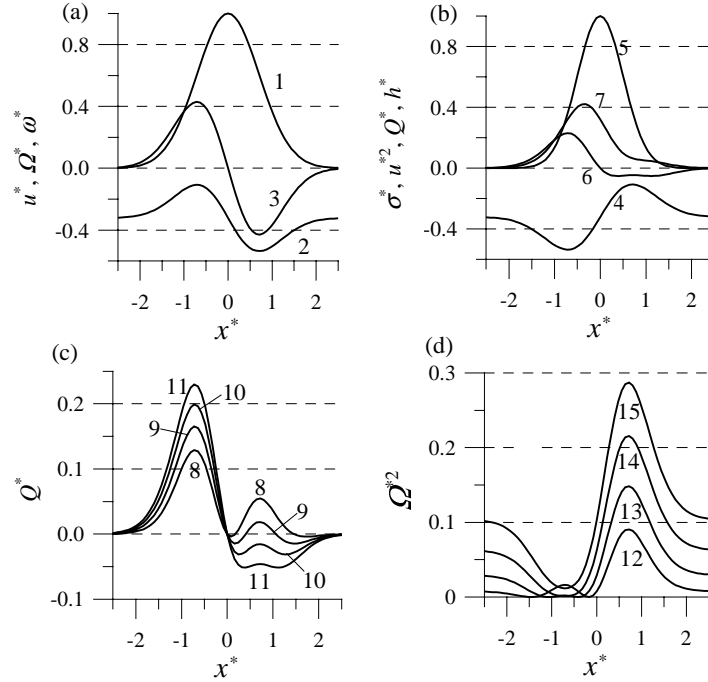


**Fig. 1.** (a) Reduced  $u^*$  (curve 1),  $\Omega^*$  (for latitude  $\vartheta=40^\circ\text{N}$ ) (curve 2), and  $\omega^*$  (curve 3); (b) reduced  $\sigma^*$  (curve 4),  $u^{*2}$  (curve 5),  $Q^*$  (curve 6), and  $h^*$  (curve 7) for latitude  $\vartheta=40^\circ\text{N}$ ; (c) reduced work  $Q^*$  for latitudes  $\vartheta=10^\circ\text{N}$  (curve 8),  $\vartheta=20^\circ\text{N}$  (curve 9),  $\vartheta=30^\circ\text{N}$  (curve 10), and  $\vartheta=40^\circ\text{N}$  (curve 11); (d) reduced  $\Omega^{*2}$  for latitudes  $\vartheta=10^\circ\text{N}$  (curve 12),  $\vartheta=20^\circ\text{N}$  (curve 13),  $\vartheta=30^\circ\text{N}$  (curve 14), and  $\vartheta=40^\circ\text{N}$  (curve 15) versus normalized transverse coordinate  $x^*$ .

ETM energy transfer. The momentum transport  $h^*$  retains its positive value and the velocity gradient has opposite signs on either side of the jet, therefore on the right the momentum appears to be transported in the upgradient direction. To show the dependence of the depicted quantities on latitude  $\vartheta$ , the profiles of  $Q^*$  and  $\Omega^{*2}$  are presented in Fig. 1c and Fig. 1d for  $\vartheta=10, 20, 30$ , and  $40^\circ\text{N}$ . The depicted profiles show an increase in the effect of the ETM energy transfer as well as in the kinetic energy of the orientated turbulence constituent ( $K^\Omega \sim \Omega^{*2}$ ) with increasing  $\vartheta$ . The maximum values of  $\Omega^{*2}$  on the right (anti-cyclonic) side of the jet exceed its values on the left (cyclonic) jet side, separated by a deep minimum of  $\Omega^{*2}$  for all latitudes. All calculations presented in Fig. 1 are performed for the northern hemisphere. When in the northern hemisphere the “negative viscosity” region is on the right side of the jet, then in the southern hemisphere it appears on the left.

Consider now the situation for finite  $\lambda$ , then the integral of Eq. (8) reads

$$\Omega^* = \lambda \int_0^{x^*} \left[ \frac{1}{\varepsilon} \frac{\kappa}{\gamma + \kappa} \sin \vartheta - \frac{\gamma}{\gamma + \kappa} \omega^* \right] \sinh(\lambda(x^* - t)) dt + C_1 \cosh \lambda x^* + C_2 \sinh \lambda x^*, \quad (17)$$

where  $C_1$  and  $C_2$  are the integration constants, determined from the condition  $\Omega^* = -\kappa \sin \vartheta / (\gamma + \kappa)$  following from (13) at an arbitrary location outside the jet area where  $\Omega^*$  is considered as not influenced by the  $\omega^*$ -field. The diffusion effect is illustrated in Fig. 2 by calculated  $\Omega^*$ ,  $\sigma^*$ , and  $Q^*$  for infinite  $\lambda$  (curves 1, 4, and 7, respectively), for  $\lambda = 1.5$  (curves 2, 5, and 8, respectively), and for  $\lambda = 0.5$  (curves 3, 6, and 9, respectively).

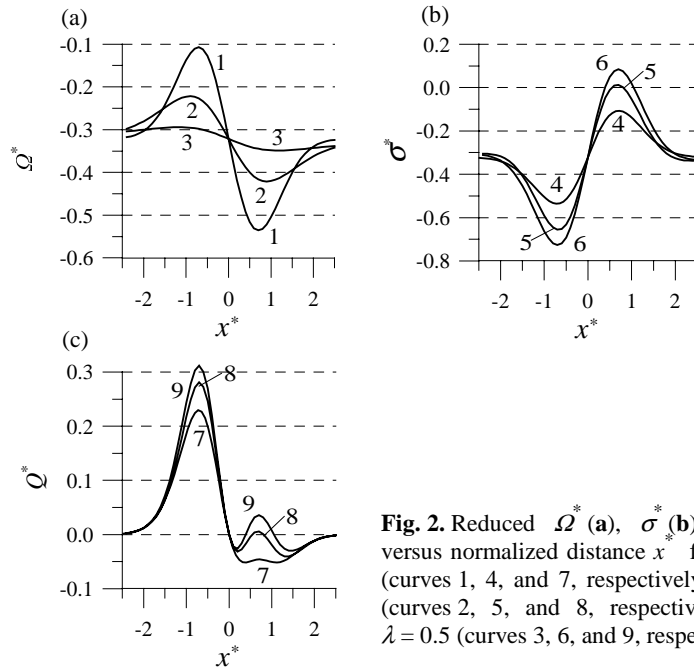


**Fig. 2.** Reduced  $\Omega^*$  (a),  $\sigma^*$  (b), and  $Q^*$  (c) versus normalized distance  $x^*$  for infinite  $\lambda$  (curves 1, 4, and 7, respectively), for  $\lambda = 1.5$  (curves 2, 5, and 8, respectively), and for  $\lambda = 0.5$  (curves 3, 6, and 9, respectively).

and for  $\lambda = 0.5$  (curves 3, 6, and 9, respectively). According to Fig. 2a, the decrease in  $\lambda$  (increase in the diffusion scale of the moment of momentum  $M$ ) is accompanied by a decrease in the amplitude of variation of  $\Omega^*$  together with an increase in the width of the region with non-zero  $\Omega^*$ . On the contrary, the decrease in  $\lambda$  is accompanied by an increase in the amplitude of  $\sigma^*$  (Fig. 2b). Finally, the decrease in  $\lambda$  is accompanied by an increase in  $Q^*$  on both sides of the jet, leading to a decrease in the effect of ETM energy transfer on the right side of the jet. On the left side of the jet the effect of the decrease in  $\lambda$  on  $Q^*$  variation is analogous to the effect of the increase in  $\vartheta$ , and on the right side the effect of the decrease in  $\lambda$  is analogous to the effect of the decrease in  $\vartheta$ .

## 5. MODEL APPLIED TO THE GULF STREAM OBSERVATIONS

The model suggested in the previous section presents the basic physical mechanism of the momentum transport and the associated energy transfer between the turbulence and the mean flow in an oceanic jet flow illustrated on the Gaussian velocity distribution. The mechanism includes the effects of momentum upgradient transport and the ETM energy transfer. The following particularizes the discussion for a realistic situation compared with the observed data in the Gulf Stream sections along latitudes 26°N (Florida Straits) and 35°N (off Onslow Bay) [12]. The calculations are performed for  $\gamma = 1.5 \kappa = 10^6 \text{ kg m}^{-1} \text{ s}^{-1}$ ,  $\lambda = 0.8$  and for the average velocity approximated by  $u = u_0(\exp(-x^{*2}) + Ax^* + B)$ , where  $x^* = x/L$ ,  $u_0 = 1 \text{ m s}^{-1}$ . For the section  $\vartheta = 35^\circ\text{N}$ , off Onslow Bay,  $L = 1.5 \times 10^4 \text{ m}$ ,  $A = 10^{-5} \text{ m}^{-1}$ ,  $B = 0.15$ , and for section  $\vartheta = 26^\circ\text{N}$ , in the Florida Straits,  $L = 1.8 \times 10^4 \text{ m}$ ,  $A = -6.9 \times 10^{-6} \text{ m}^{-1}$ ,  $B = 1.2$ . The calculated profiles of  $\sigma_{xy} = \gamma \kappa u_0 \sigma^* / (\gamma + \kappa)L$  along latitudes 35°N (off Onslow Bay) and 26°N (Florida Straits), together with the estimated values of the time average quantity  $-\rho \overline{v'_x v'_y}$ , are presented in Fig. 3a and Fig. 4a. Despite of the rough velocity approximations applied, the similarity between data and calculations is remarkable. It concerns not only the dependence of  $\sigma_{xy}$  on  $x^*$  but also on  $\vartheta$ .

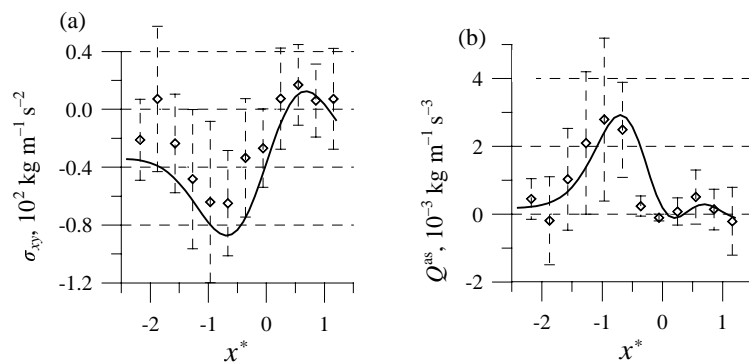


**Fig. 3.** The measured (diamonds) and modelled (curves)  $\sigma_{xy}$  (a) and  $Q^{\text{as}}$  (b) versus normalized transverse distance  $x^*$  in the Gulf Stream along  $\vartheta = 35^\circ\text{N}$  (off Onslow Bay).

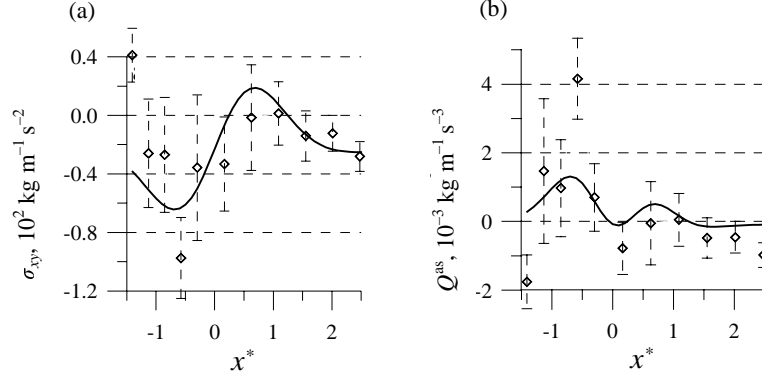


**Fig. 4.** The measured (diamonds) and modelled (curves)  $\sigma_{xy}$  (a) and  $Q^{\text{as}}$  (b) versus normalized transverse distance  $x^*$  in the Gulf Stream along  $\vartheta = 26^\circ\text{N}$  (Florida Straits).

The similar behaviour of the calculated  $\sigma_{xy}$  and the measured  $-\overline{\rho v'_x v'_y}$  in Fig. 3a and Fig. 4a suggests the interpretation of  $-\overline{\rho v'_x v'_y}$  data as measured values of  $\sigma_{xy}$ . According to the interpretation and due to  $\sigma_{yx} = -\sigma_{xy}$  in the suggested model, we get  $\sigma_{yx} = \overline{\rho v'_x v'_y}$ . As a consequence,

$$Q = Q^{\text{as}} = \sigma_{yx} u_{,x} = \overline{\rho v'_x v'_y u_{,x}}. \quad (18)$$

The modelled  $Q^{\text{as}}$  (curves in Fig. 3b and Fig. 4b), together with the values of  $Q$  estimated from the measured velocity and  $-\overline{\rho v'_x v'_y}$  data (diamonds in Fig. 3b and Fig. 4b), show the domination of the mean-to-eddy energy transfer,  $Q > 0$ , over both jet sections.

Consider now the jet from the point of view of the CTM. Then  $\sigma_{xy} = \sigma_{yx}$  and instead of (18) we would have  $Q = Q^{\text{s}} = \sigma_{yx} u_{,x} = -\overline{\rho v'_x v'_y u_{,x}}$  [1]. Therefore, when interpreted within the CTM, the ETM energy transfer would dominate in the jet area. This interpretation would presume a powerful constant source of turbulence energy in the region. The absence of such an energy source proves the CTM as failing to describe the energy and momentum balance data measured within the Gulf Stream.

## 6. CONCLUSIONS

The failure of the CTM to explain the upgradient momentum transport and the associated ETM energy transfer in the turbulent flow challenges the researchers to looking for adequate mechanisms forcing the momentum transport in turbulent flows. This paper suggests a mechanism accounting for the eddy rotation orientation (the RAT theory). The mechanism is realized in the suggested model of a geophysical jet flow. The model gives a natural explanation to the significant differences in the turbulence regimes on the cyclonic and anticyclonic sides of

the jet. The model skill is tested on the data measured in the Gulf Stream sections along 26°N (Florida Straits) and 35°N (off Onslow Bay). It is shown that, unlike the interpretation of the observed data within the CTM, the interpretation of the measured data within the suggested model does not presume the negative viscosity.

## REFERENCES

1. Starr, V. P. *Physics of Negative Viscosity Phenomena*. McGraw-Hill, New York, 1968.
2. Morimoto, H. and Maekawa, T. Negative viscosity induced in a ferromagnetic colloidal system subjected to both external shear flow and ac magnetic fields. *Int. J. Modern Phys. B*, 2002, **16**, 2610–2615.
3. Bacri, J.-C., Perzynski, R., Shliomis, M. I. and Burde, G. I. “Negative-viscosity” effect in a magnetic fluid. *Phys. Rev. Lett.*, 1995, **75**, 2128–2131.
4. Smoljakov, A. I., Diamond, P. H. and Malkov, M. Coherent structure phenomena in drift wave-zonal flow turbulence. *Phys. Rev. Lett.*, 2000, **80**, 491–494.
5. Heinloo, J. *Phenomenological Mechanics of Turbulence*. Valgus, Tallinn, 1984 (in Russian).
6. Heinloo, J. *Turbulence Mechanics. Introduction to General Theory of Turbulence*. Estonian Academy of Sciences, Tallinn, 1999 (in Russian).
7. Heinloo, J. The formulation of turbulence mechanics. *Phys. Rev. E*, 2004, **69**, 056317.
8. Webster, T. F. The effects of meanders on the kinetic energy balance of the Gulf Stream. *Tellus*, 1961, **13**, 392–401.
9. Lin, G. and Atkinson, J. A mechanism for offshore transport across the Gulf Stream. *J. Phys. Oceanogr.*, 2000, **30**, 225–232.
10. Toompuu, A., Heinloo, J. and Soomere, T. Modelling of the Gibraltar Salinity Anomaly. *Oceanology*, 1989, **29**, 698–702 (English translation).
11. Heinloo, J. and Võsumaa, Ü. Rotationally anisotropic turbulence in the sea. *Ann. Geophys.*, 1992, **10**, 708–715.
12. Võsumaa, Ü. and Heinloo, J. Evolution model of the vertical structure of the active layer of the sea. *J. Geophys. Res.*, 1996, **101**, 25635–25646.
13. Heinloo, J. and Toompuu, A. Antarctic Circumpolar Current as a density-driven flow. *Proc. Estonian Acad. Sci. Phys. Math.*, 2004, **53**, 252–265.
14. Heinloo, J. Eddy-driven flows over varying bottom topography in natural water bodies. *Proc. Estonian Acad. Sci. Phys. Math.*, 2006, **55**, 235–245.
15. Heinloo, J. and Toompuu, A. Modelling a turbulence effect in formation of the Antarctic Circumpolar Current. *Ann. Geophys.*, 2006, **24**, 3191–3196.
16. Truesdell, C. A. *The Elements of Continuum Mechanics*. Springer, New York, 1966.
17. Sedov, L. I. *A Course in Continuum Mechanics*. Kluwer, 1987.
18. Eringen, A. C. and Chang, T. S. Micropolar description of hydrodynamic turbulence. *Recent Adv. Engng. Sci.*, 1970, **5**, 1–8.
19. Peddieson, J. An application of the micropolar fluid model to the calculation of turbulent shear flow. *Int. J. Eng. Sci.*, 1992, **10**, 23–32.
20. Eringen, A. C. Micromorphic description of turbulent channel flow. *J. Math. Anal. Appl.*, 1972, **39**, 253–256.
21. Nikolaevskiy, V. N. *Angular Momentum in Geophysical Turbulence: Continuum Spatial Averaging Method*. Kluwer, 2003.
22. Dahler, J. S. and Scriven, L. F. Angular momentum of continua. *Nature*, 1961, **192**, 36–37.
23. Dahler, J. S. Transport phenomena in a fluid composed of diatomic molecules. *J. Chem. Phys.*, 1959, **30**, 1447–1475.
24. Eringen, A. C. Theory of micropolar fluids. *Math. and Mech.*, 1966, **16**, 1–18.

25. Ariman, T., Turk, M. A. and Silvester, D. O. Microcontinuum fluid mechanics – review. *Int. J. Eng. Sci.*, 1973, **11**, 905–930.
26. Richardson, O. *Weather Prediction by Numerical Process*. Cambridge University Press, 1922.
27. Kolmogoroff, A. N. The local structure of turbulence in incompressible viscous fluids for very large Reynolds numbers. *C. R. Acad. Sci. URSS*, 1941, **30**, 376–387.
28. Sagaut, P. *Large Eddy Simulation for Incompressible Flows*. Springer-Verlag, 2006.
29. Lesieur, M., Métais, O. and Comte, P. *Large-Eddy Simulations of Turbulence*. Cambridge University Press, Cambridge, 2005.
30. Volker, S., Venugopal, P. and Moser, R. D. Optimal large eddy simulation of turbulent channel flow based on a direct numerical simulation statistical data. *Phys. Fluids*, 2002, **14**, 3675–3692.
31. O'Dwyer, J., Williams, R. G., Lacasce, J. H. and Speer, K. G. Does the potential vorticity distribution constrain the spreading of floats in the North Atlantic? *J. Phys. Oceanogr.*, 2000, **30**, 721–732.
32. Pedlosky, J. *Geophysical Fluid Dynamics*. Springer-Verlag, 1982.

## **Energia ülekanne pööristelt keskmisele liikumisele geofüüsikalistes turbulentsetes jugades**

Jaak Heinloo ja Aleksander Toompuu

On käsitletud energia ülekannet turbulentses keskkonnas. Käsitlus tugineb pöördeliselt mitteisotroopse turbulentsi teooriale (PMT-teooria). On näidatud, et PMT-teooria võimaldab selgitada energia ülekannet turbulentses keskkonnas selle turbulentselt komponendilt keskmistatud liikumisele. Formuleeritud käsitlus ei vaja negatiivse turbulentsi viskoossuskoeffitsiendi rakendamist, mis on omane probleemi käsitlusele turbulentsi mehaanika senise formuleeringu raames. Artiklis tuletatud teoreetilised väited on konkretiseeritud geofüüsikalise joalise voolamise juhule. Golfi hoovuse ristlõigetes laiustel 26°N (Florida väinad) ja 35°N (Onslow' laht) mõõdetud andmetele tuginedes on näidatud, et formuleeritud mudel on heas kooskõlas mõõdetud andmetega, kusjuures andmete interpretatsioon pakutud mudeli raames osutub oluliselt erinevaks nende interpretatsioonist turbulentsi liikumise mehaanika senise formuleeringu raames.